



Crust recycling in the sources of two parallel volcanic chains in Shandong, North China

Gang Zeng^a, Li-Hui Chen^{a,*}, Albrecht W. Hofmann^{b,c}, Shao-Yong Jiang^a, Xi-Sheng Xu^a

^a State Key Laboratory for Mineral Deposits Research, School of Earth Sciences and Engineering, Nanjing University, Nanjing 210093, China

^b Max-Planck-Institut für Chemie, Postfach 3060, D-55020 Mainz, Germany

^c Lamont-Doherty Earth Observatory of Columbia University, P.O. Box 1000, Palisades, NY 10964, USA

ARTICLE INFO

Article history:

Received 23 June 2010

Received in revised form 7 December 2010

Accepted 8 December 2010

Available online 8 January 2011

Editor: R.W. Carlson

Keywords:

alkaline basalts

intra-continental volcanic chains

crustal recycling

lower continental crust

lithosphere thickness

ABSTRACT

Recycled crustal components have been documented for many sources of hotspot-related ocean island basalts, but they have been difficult to identify in continental basalts, because in continental settings, hotspots are often obscured and recycled crustal sources are difficult to distinguish from crustal contamination. We show major, trace element and Sr–Nd–Hf isotopic compositions for two parallel chains of Cenozoic volcanoes from Shandong Province, North China, which are free of crustal contamination and show clear evidence for recycling of mafic lower crust. Sr, Nd, and Hf isotopes in the two volcanic chains form separate binary mixing arrays, which converge on the composition of Dashan, an isolated, nephelinitic volcano with the most depleted isotopic signature. The two chains have lower CaO values and significantly diverging isotope enrichment trends from this common endmember. Both trends deviate from the normal Sr–Nd and Hf–Nd mantle array toward lower $^{87}\text{Sr}/^{86}\text{Sr}$ and higher ε_{Hf} values, all features that point to a (recycled) eclogitic source.

We invoke a two-stage evolution model to generate the endmembers of these two mixing trends. In the first stage, recycled mafic crust (eclogite) is depleted by earlier (late Mesozoic) melt extraction, which elevates the Lu/Hf of the residue relative to Sm/Nd due to garnet control during melting. Subsequently, these silica-deficient residues are transported to the deeper mantle. Finally, in Cenozoic time, upwelling mantle (possibly a plume) transports lenses of residual eclogites into the shallow asthenosphere. The recycled crustal components beneath the two chains differ somewhat in isotopic composition due to different degree of the earlier melting. The upwelling mantle spreads beneath the lithosphere and flows toward regions of thinned lithosphere, e.g. the Tan–Lu Fault Zone in North China, where the recycled crust undergo remelting and mix with peridotite-derived melts to produce the two mixing trends observed.

© 2010 Elsevier B.V. All rights reserved.

1. Introduction

The origin of wide-spread Cenozoic continental volcanism in eastern China is problematic because there is no obvious cause of melting, since only some of this volcanism is directly associated with rifting. Recent seismic tomography has identified a low velocity region in the upper mantle beneath the central part of the North China craton (NCC), reaching at least into the transition zone (Zhao et al., 2009), and this might represent a mantle plume. However, much of the volcanism is located hundreds of kilometers from this possible plume, and invoking a plume mechanism to account for all these melts might initially seem far-fetched. We will nevertheless argue that this represents perhaps the simplest mechanism for causing significantly older, recycled crustal material to melt and generate some of the Cenozoic magmatism discussed in this paper.

Major Cenozoic basaltic fields in the NCC include Hannuoba, Datong, Taihang, and Shandong. Previous studies suggest that alkaline basalts in the NCC have an asthenospheric source by their OIB-like geochemical and isotopic compositions, whereas the tholeiites may have been contaminated by the crust or the lithospheric mantle because of their more enriched isotopic compositions (Peng et al., 1986; Song et al., 1990; Xu et al., 2005). Tang et al. (2006) proposed that the geochemical signatures of alkaline basalts in Taihang, in particular their moderately enriched isotopic compositions, can be induced by asthenosphere–lithosphere interactions. Other authors have attributed the OIB-like signatures of alkaline basalts to the contributions of the recycled crust in their asthenospheric source (Chen et al., 2009a; Liu et al., 2008). In addition, our recent study of the basanites and nephelinites from Shandong has suggested that their asthenospheric source has been enriched by carbonatitic liquids (Zeng et al., 2010). Therefore, the nature of the source(s) of Cenozoic alkaline basalts in the NCC remains controversial, and the specific cause of melting has hardly been addressed in the recent literatures.

We focus here on a specific example of two parallel volcanic chains in the eastern part of the NCC, which superficially resemble the

* Corresponding author.

E-mail address: chenlh@nju.edu.cn (L.-H. Chen).

parallel volcanic chains on the Hawaiian islands, in that they are parallel, spaced about 40 km apart, and display consistent geochemical differences in a manner somewhat analogous to those described for the Kea and Loa trend volcanic chains on Hawaii (Abouchami et al., 2000; Abouchami et al., 2005). And although there are many obvious differences as well, such as the lack of time progression, the absence of an immediately obvious plume source, and a rather short length of the chains (50 km), there are additional similarities, such as inferred source compositions containing recycled crustal components, which are noteworthy. We show that the low-Ca contents of primary magmas are derived from an eclogitic source component, which is thought to be derived from older, recycled lower continental crust. These residual eclogite-derived melts are mixed with nephelinitic melts derived from a peridotitic source, which is also present in many of the isolated volcanic centers on the NCC.

Ebinger and Sleep (1998) proposed that much of the young volcanism occurring in Africa is related to a single plume rising in the Afar region and laterally flowing to shallow asthenospheric regions beneath thinned lithosphere, and we will argue that a similar mechanism can account for much of the Cenozoic volcanism in northern China. When the sublithospheric plume flow encounters regions of locally thinned lithosphere, it reaches sufficiently shallow levels to undergo melting and produce the observed chains of basaltic volcanoes. Thus we suggest that the consistent geochemical differences between the two volcanic chains are related to heterogeneities that have been severely stretched and elongated by plume flow, in a manner similar to those observed in the Hawaiian plume by Abouchami et al. (2005) and modeled by Farnetani and Hofmann (2010).

2. Geological setting and sample description

The North China Craton (NCC) is one of the world's oldest cratons, located in the central part of eastern China (Figure 1). The NCC is

composed of two Archean blocks (the eastern block, and the western block) and one Proterozoic orogenic belt (the central part) (Figure 1) (Zhao et al., 2005). Cenozoic alkaline basalts in the NCC, as well as those in northeast and southeast China, represent the youngest magmatism in eastern China, and provide an ideal opportunity to study the chemical heterogeneities of the asthenosphere beneath a continent (see reviews by Chen et al., 2009a; Zou et al., 2000; and references therein) (Figure 1). The Shandong Province is located in the southeast of the NCC. The Cenozoic alkaline magmatism in Shandong took place during two periods: 24.0–10.3 Ma and 8.7–0.3 Ma (see the review by Luo et al., 2009). The early magmatism was profuse and characterized by large volcanoes densely distributed in a narrow area near the Tan–Lu Fault Zone (TLFZ) (Figure 1); the rocks of this age are mainly weakly alkaline basalts, including alkali olivine basalts and basanites. The later magmatism is characterized by small, isolated volcanoes, widely scattered in areas far from the TLFZ; the rocks of this group are dominated by basanites and nephelinites (Zeng et al., 2010), e.g. Dashan in Wudi. Mantle xenoliths are commonly contained in the alkaline basalts from Shandong. In particular, the early weakly alkaline basalts are arranged in two parallel volcanic chains: the north chain and the south chain (Figure 1). The parallel volcanic chains show a direction of north by east 55°, and the angle between these volcanic chains and the TLFZ is about 40°. They range about 40 km in length, and the distance between them is about 50 km.

We have chosen eight volcanoes from the two chains, including Niushan, Shanwang, Taohuashan, Fangshan, Fuyanshan of the north chain and Longshan, Chengdingshan, Liushan of the south chain, to study the genesis of basalts from chain-related volcanoes in Shandong. Samples from Niushan, Shanwang, Taohuashan, Chengdingshan and Fuyanshan are unaltered. Samples from Fangshan, Longshan, and Liushan are slightly altered, and olivine phenocrysts are partially altered to low-temperature iddingsite. All samples have minor olivine (<15%) as phenocrysts set in a groundmass of olivine,

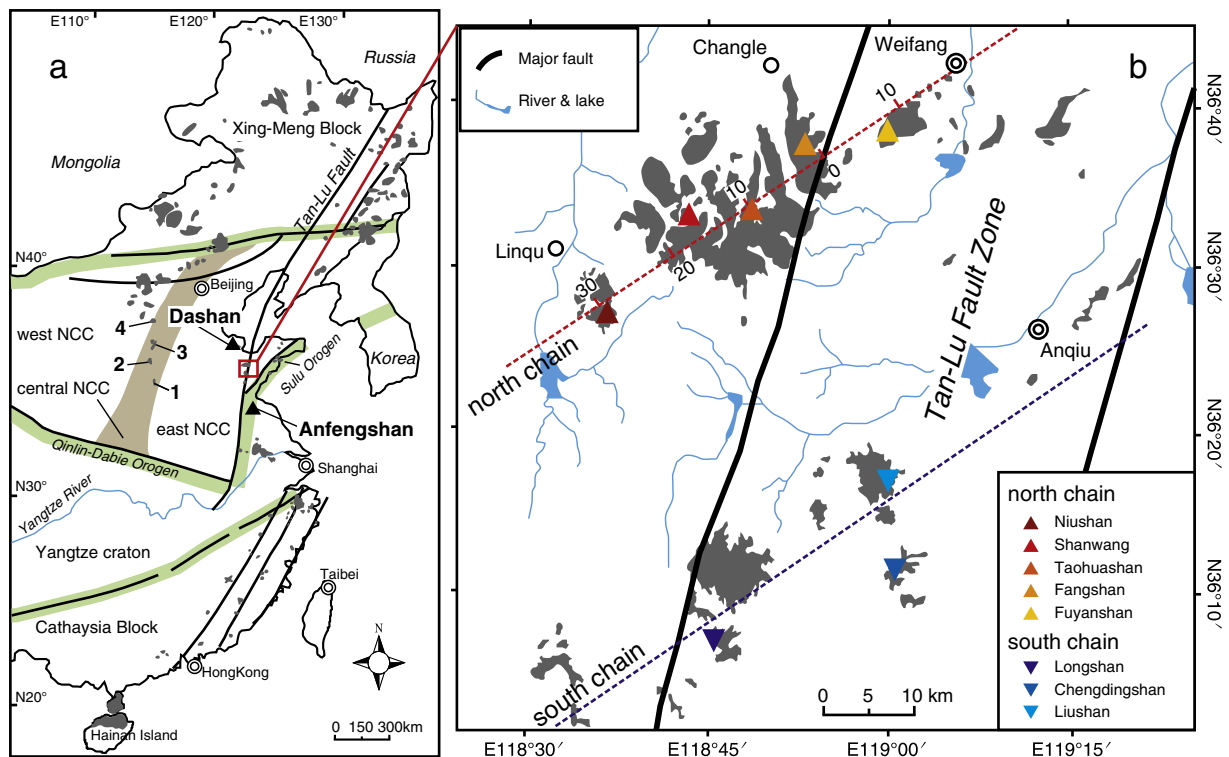


Fig. 1. (a) Simplified geological map of eastern China. Cenozoic basalts from Taihang Mountain area of central NCC include: 1 – Hebi basalts (4.3–4.0 Ma), 2 – Zuozhan basalts (5.6 Ma), 3 – Xiyang–Pingding basalts (7.9–7.3 Ma), and 4 – Fanshi basalts (26–24 Ma) (Liu et al., 1992; Tang et al., 2006). (b) Distribution of the Cenozoic chain-forming volcanoes in Shandong. The red line and the blue line refer to the distributing directions of the north chain and the south chain, respectively. The distributions of Cenozoic basalts in eastern China and in Shandong are from Liu et al. (1992) and Shandong Institute of Geological Survey (2005), respectively.

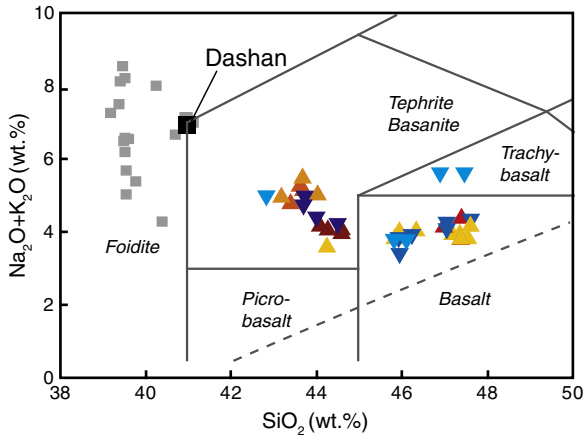


Fig. 2. Variations in $\text{Na}_2\text{O} + \text{K}_2\text{O}$ vs. SiO_2 for chain-related basalts in Shandong and an example of isolated volcanism, represented by the Dashan nephelinite. Other strongly alkaline basalts from isolated volcanoes in Shandong (Zeng et al., 2010) are shown as gray squares. Dashan stands for the average values of Dashan nephelinites. Symbols for chain-related basalts in Shandong are the same as in Figure 1b.

Ti-magnetite, and glass. Neither plagioclase nor pyroxene phenocrysts are observed in these samples.

3. Geochemical results

We measured major oxides, trace elements, and Sr, Nd, Hf isotopes for chain-related basalts in Shandong. The analytical methods are given in Appendix A and the results are shown in the Table S1. For comparison, the average values of major oxides, trace elements, and Sr, Nd, Hf isotopes of the nephelinites from Dashan, as a representative of the strongly alkaline, small, and isolated volcanoes in Shandong, are also shown in the Table S1.

Compared with the isolated volcano samples from Shandong (e.g. Dashan nephelinites), the basalts from two parallel volcanic chains

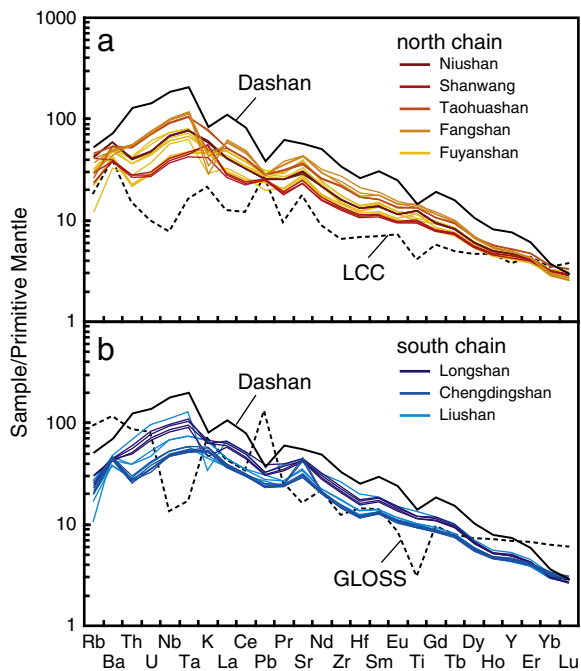


Fig. 3. Primitive-mantle normalized incompatible element diagram for chain-related basalts in Shandong. Dashan stands for the average values of Dashan nephelinites. Data for Global Subducting Sediment (GLOSS) and lower continental crust (LCC) are from Plank and Langmuir (1998) and Rudnick and Gao (2003), respectively. The primitive mantle values are from McDonough and Sun (1995).

have higher SiO_2 (42.8–47.6 wt.%), lower TiO_2 (1.8–3.0 wt.%) and alkalis ($\text{Na}_2\text{O} + \text{K}_2\text{O} = 3.0\text{--}5.5$ wt.%) contents. According to the nomenclature of (Le Bas et al., 1986), they are classified as basanites to alkali olivine basalts, with only two samples plotting in the area of trachybasalts (Figure 2). There are obvious negative correlations between TiO_2 vs. SiO_2 , and P_2O_5 vs. SiO_2 (not shown). No correlation is observed between SiO_2 and other oxides. The chondrite-normalized patterns of these chain-related rocks are characterized by a moderate LREEs enrichment ($\text{La}/\text{Yb} = 12.6\text{--}33.3$), without Eu or Ce anomalies (not shown). In a primitive-mantle normalized incompatible element diagram (Figure 3), these basalts resemble many ocean island basalts in terms of enrichment in Nb and Ta, relative to LREEs. Except for the basalts from Shanwang and a few samples from Liushan, most samples show slightly negative Pb anomalies. The range of their Ce/Pb ratios (9.9–19.6) is lower than OIB ($\approx 25 \pm 5$) (Hofmann et al., 1986), and show a negative correlation with Ce/La ratios (Figure 4). In addition, these chain-related basalts show obviously lower Th/La ratios (0.09–0.13) than those isolated volcano samples from Shandong ($\text{Th}/\text{La} = 0.13\text{--}0.17$) and average continental crust (Figure 5). The average Th/La ratios of the continental crust, the upper continental crust, and the lower continental crust are 0.28, 0.34, and 0.15, respectively (Rudnick and Gao, 2003).

In general, these chain-related basalts have moderately depleted or near-bulk-earth Sr, Nd, and Hf isotopic compositions (Figure 6a, b), and show a negative correlation in the plot of ϵ_{Nd} vs. $^{87}\text{Sr}/^{86}\text{Sr}$, and a positive correlation in the plot of ϵ_{Nd} vs. ϵ_{Hf} , respectively (Figure 6c, d). The differences in isotopes are also reflected by differences in lithology. The alkali olivine basalts show more enriched isotopic compositions than do basanites (Figure 7a). In addition, small-scale, but systematic isotopic differences between samples from the two volcanic chains (Figure 6c, d), associated with differences in Zr/Hf ratios (Figure 7b), are revealed clearly. The isotopic arrays of the two volcanic chains are similar and share the depleted endmember (lower $^{87}\text{Sr}/^{86}\text{Sr}$ ratios and higher ϵ_{Nd} , ϵ_{Hf} values), which has similar Sr, Nd, Hf isotopes to that of Dashan nephelinites. Both trends deviate from the normal terrestrial Hf–Nd correlation by having lower slopes and pointing to endmembers with relatively high ϵ_{Hf} values at a low ϵ_{Nd} value. However, in detail, the isotope correlations of two chains differ increasingly with decreasing ϵ_{Nd} values. For a given ϵ_{Nd} value, the north chain has higher $^{87}\text{Sr}/^{86}\text{Sr}$ ratios and lower ϵ_{Hf} values than the south chain.

Remarkably, there are two distinct arrays in the plots of Lu/Hf and Sm/Yb ratios vs. ϵ_{Hf} (Figure 7c, d). One array is characterized by a negative correlation of Lu/Hf vs. ϵ_{Hf} values and positive correlation of

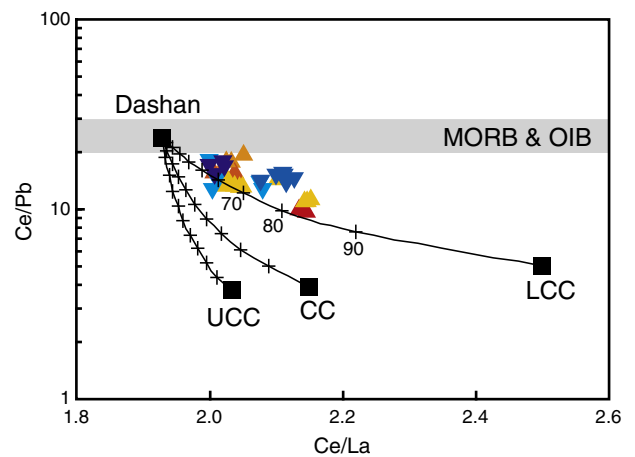


Fig. 4. Variations in Ce/Pb vs. Ce/La for chain-related basalts in Shandong. Data for CC (continental crust; Ce = 43, Pb = 11, La = 20), UCC (upper continental crust; Ce = 63, Pb = 17, La = 31) and LCC (lower continental crust, Ce = 20, Pb = 4, La = 8) are from Rudnick and Gao (2003). Fields of MORB and OIB are after Hofmann et al. (1986). Symbols for chain-related basalts in Shandong are the same as in Figure 1b.

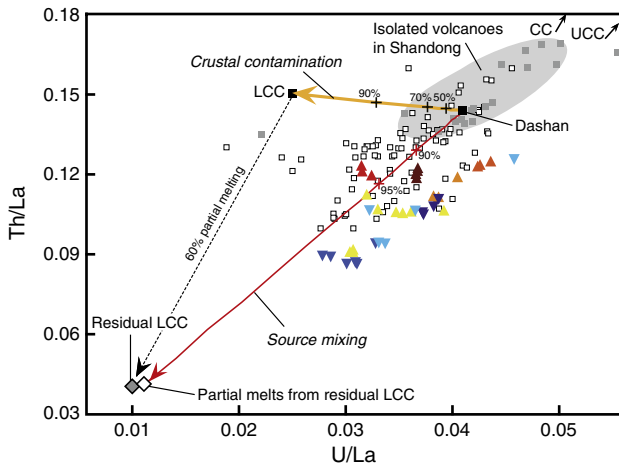


Fig. 5. Variations in Th/La vs. U/La for chain-related basalts in Shandong and modeling for their genetic relationship. The average Th/La and U/La ratios of CC (Th/La = 0.28, U/La = 0.065), UCC (Th/La = 0.34, U/La = 0.087) and LCC (Th/La = 0.15, U/La = 0.025) are from Rudnick and Gao (2003). At 130 Ma, 60% partial melting decreases the Th/La ratio of the recycled LCC (eclogite) from 0.150 to 0.036, and its U/La ratio decreases from 0.025 to 0.010. At 20 Ma, the residue of recycled LCC (eclogite) remelted (15% proportions of melts extracted), and these melts mix with nearby peridotite-derived melts to produce the basalts from two parallel volcanic chains in Shandong. The partition coefficients used are: for garnet, Th = 0.002, U = 0.006, La = 0.001; and for clinopyroxene, Th = 0.007, U = 0.008, La = 0.034 (Klemme et al., 2002). The proportions of residual phase during melting is assumed to be modal (with 40% garnet and 60% clinopyroxene in the first melting; 0% garnet and 100% clinopyroxene in the second melting). Dashan stands for the average values of Dashan nephelinites. The alkaline basalts from isolated volcanoes in Shandong (gray squares) are from Zeng et al. (2010). Unfilled squares stand for Cenozoic basalts from other places in North China (Liu et al., 2008; Tang et al., 2006; Xu et al., 2005; Zhang et al., 2009). Symbols for chain-related basalts in Shandong are the same as in Figure 1b.

Sm/Yb vs. ε_{Hf} values, while the other array is characterized by variable element ratios with constant ε_{Hf} values. Dashan nephelinites plot close to the high- ε_{Hf} intersection of these two arrays.

4. Discussion

As noted above, the basalts from the volcanic chains in Shandong show obvious geochemical diversity, and the correlations observed in these samples indicate the mixing of three distinct components (Figs. 6 and 7). In the isotope plots, the two arrays intersect roughly at the locus of Dashan nephelinites (Figure 6c, d). This suggests that the two chains share a common depleted endmember in their mantle sources, a component similar to that of Dashan nephelinites. Dashan nephelinites, as well as rocks from other isolated volcanoes in Shandong, have a geochemical fingerprint of high Ca/Al ratios, enrichment of most incompatible elements, superchondritic Zr/Hf ratios, and negative K, Zr, Hf, and Ti anomalies. These alkaline rocks have been proposed to be derived from low-degree melting of carbonated peridotite in the asthenospheric mantle (Zeng et al., 2010). Both of the other components (the enriched endmembers) of the two chains have lower ε_{Nd} , ε_{Hf} values and higher $^{87}\text{Sr}/^{86}\text{Sr}$ ratios than the depleted endmember (Figure 6). Materials from these enriched endmembers have higher SiO_2 contents and lower Zr/Hf ratios than those from the depleted endmember (Figure 7a, b). In the following sections, we shall discuss the origin of such enriched endmembers.

4.1. Crustal contamination?

These chain-related basalts have high MgO (7.7–11.7 wt.%), Ni (135–270 ppm) contents (Table S1), suggesting insignificant fractional crystallization of olivine. There is no observable correlation between MgO and Cr, as well as their high Cr contents (222–

352 ppm), suggesting negligible fractional crystallization of pyroxene for these chain-related basalts. The lack of a negative Eu anomaly (not shown) suggests no significant removal of plagioclase. Therefore, most of these alkaline basalts have the features of near primary melts, and their geochemical compositions can be used to infer their genesis.

The lower Ce/Pb ratios (9.9–19.6) indicate these melts might have been contaminated by crustal components (Figure 4). As we know, there is a nice positive correlation in the plot of $^{143}\text{Nd}/^{144}\text{Nd}$ vs. $^{206}\text{Pb}/^{204}\text{Pb}$ for Cenozoic basalts from North China (see reviews by Chen et al., 2009a and Zou et al., 2000), including Cenozoic basalts from Shandong (Peng et al., 1986), and the enriched component has unradiogenic lead isotopes, which supports the proposal of an ancient lower continental crust as the enriched endmember (Chen et al., 2009a). In the plot of Ce/Pb vs. Ce/La, simple mixing calculations between Dashan nephelinites and the average bulk continental crust (including lower crust, upper crust and total crust) suggest that the lower continental crustal material (40–80%) is the most suitable candidate for the enriched component(s) of the chain-related basalts (Figure 4). Therefore, a simple model for the explanation of the isotopic variation is that these basalts have been contaminated by lower continental crust in their ascending way.

However, besides of their geochemical features of primary melts (high MgO, Ni, and Cr), there are several lines of evidence against such contamination model. Firstly, mantle xenoliths are common in both two volcanic chains, which suggests that the host magma are low-viscosity melts and ascend rapidly, and thus seems hardly to be contaminated by lower continental crust with the high proportion of 40–80% (as shown in Figure 4). Secondly, Dashan nephelinites, as well as other isolated volcanoes in Shandong, have high Th/La ratios (average 0.14 for Dashan). However, the chain-related basalts show obviously lower Th/La ratios (0.09–0.13), which cannot be evolved from Dashan-like magma by contamination of lower continental crust (average 0.15) (Figure 5). Thirdly, most of these chain-related basalts have lower CaO contents (8.2–10.0 wt.%) than those of experimentally produced peridotite-derived melts (CaO = 10.0 wt.%) (Herzberg, 2006) (Figure 8). Lower continental crust, with average CaO content of 9.6 wt.%, is not a suitable contaminant for such CaO-depleted melts. Therefore, simply model of peridotite-derived melts contaminated by lower continental crust is not favored for the genesis of these chain-related basalts in Shandong.

4.2. Evidence for recycled lower continental crust

Previous studies of Cenozoic basalts in the NCC have suggested several candidates in the mantle as the enriched endmember to explain their geochemical and isotopic compositions, such as recycled lower continental crust (Chen et al., 2009a; Liu et al., 2008), and sub-continental lithospheric mantle (SCLM) (Tang et al., 2006; Xu et al., 2005), and the specific nature of these basalt sources is still controversial. The SCLM beneath the TLFZ has obviously more depleted isotopic characteristics (represented by the isotopic compositions of peridotite xenoliths in this area) (Chu et al., 2009; Xiao et al., 2010) (Figure 6a, b) and cannot be the enriched source of the chain-related volcanoes. Remarkably, in the plot of ε_{Nd} vs. ε_{Hf} (Figure 6d), these basalts show trends that deviate from the general mantle array at decreasing ε_{Nd} and ε_{Hf} . In principle, the involvement of subducted oceanic sediments (GLOSS) with high ε_{Hf} values might explain such a decoupling of ε_{Hf} from ε_{Nd} . However, their high $^{87}\text{Sr}/^{86}\text{Sr}$ ratios (Plank and Langmuir, 1998) make such sediments unsuitable candidates for the enriched sources of these basalts (Figure 6a). Therefore, we argue that recycled lower continental crust is a more suitable candidate for the enriched endmember(s).

When mafic lower continental crust materials are recycled into the mantle by subduction or delamination, these mafic rocks transform into SiO_2 -oversaturated eclogites. Such eclogite may melt first and produce high- SiO_2 melts, and the residues are changed into silica-deficient

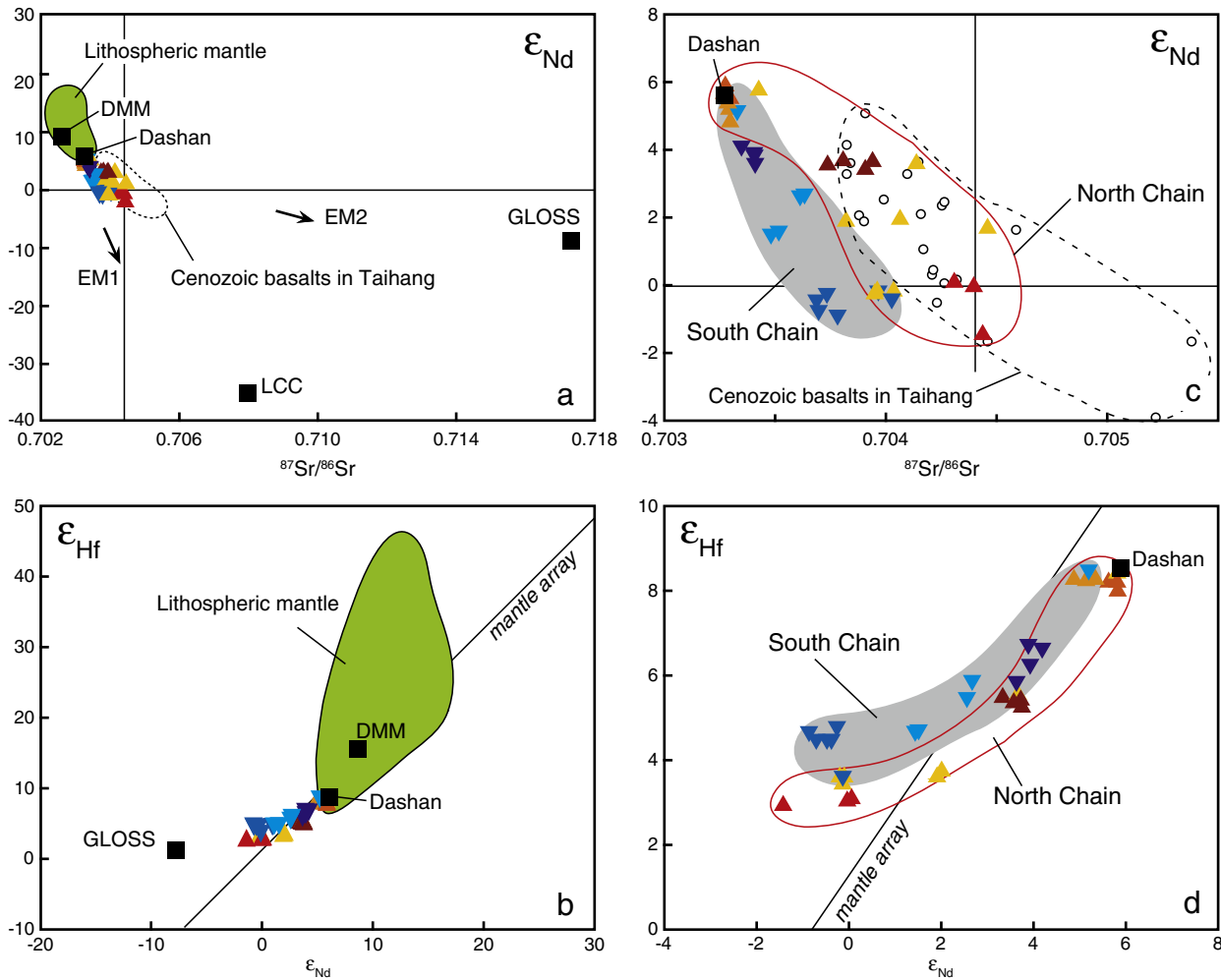


Fig. 6. Variations in ϵ_{Nd} vs. $^{87}Sr/^{86}Sr$ and ϵ_{Hf} vs. ϵ_{Nd} for chain-related basalts in Shandong. Unfilled circles stand for Cenozoic basalts from Taihang Mountain area, including Fansi, Xiyang–Pingding and Zuoquan (Tang et al., 2006). The fields of lithospheric mantle are represented by peridotite xenoliths from Cenozoic basalts in Shanwang (Chu et al., 2009) and Beiyuan (Xiao et al., 2010), two xenolith localities located in the north chain of Shandong. Data for LCC, GLOSS and DMM (depleted MORB mantle) is from Jahn et al. (1999), Plank and Langmuir (1998) and Workman and Hart (2005), respectively. The trends for EM-I and EM-II are from Zindler and Hart (1986). The mantle reference line is from Chauvel et al. (2008). Dashan stands for the average values of Dashan nephelinites. Symbols for chain-related basalts in Shandong are the same as in Figure 1b.

eclogites (Hirschmann et al., 2003; Kogiso et al., 2003; Pertermann and Hirschmann, 2003a, b; Yaxley and Green, 1998). Melting of such silica-deficient residues can produce SiO_2 -undersaturated melts suggested by previous melting experiments (Hirschmann et al., 2003; Kogiso and Hirschmann, 2006; Kogiso et al., 2003). In addition, melts from such residues are also suggested to be deficient in CaO contents because clinopyroxene is a primarily residual phase in the source (Herzberg and Asimow, 2008). In contrast, primary melts from peridotite at pressures up to 7 GPa have significantly higher CaO contents (≈ 10 wt.%), regardless of the degree of fertility of the peridotites being melted (Herzberg, 2006). The low CaO contents (8.2–10.0 wt.%) of these chain-related basalts (Figure 8) supports a clinopyroxene-rich residue rather than a peridotitic residue in the source. Therefore, the recycled lower crust (eclogitic residue) is an appropriate enriched end-member of the basalts from the chain-related volcanoes in Shandong.

The other important observation is the decoupling of ϵ_{Hf} from ϵ_{Nd} (Figure 6d). This must have been induced by an earlier stage of melting of recycled crust (to provide the time needed for the isotopic differences to develop). According to the model of Chen et al. (2009a) and Liu et al. (2008), the recycled eclogites that remained in the mantle beneath the NCC, which have been proposed to originate from subducted lower crust of Yangtze craton (Zhang et al., 2002) or delaminated lower crust of the NCC (Gao et al., 2004, 2008), were subjected to partial melting and melt extraction around 130 Ma ago.

In our very simple (batch) melt extraction model, using subducted lower crust of the Yangtze craton as an example (Figure 9), high melt fractions (55% and 60%) were extracted from the recycled eclogites. Melting of such garnet-rich rocks increased their $^{176}Lu/^{177}Hf$ ratios (from 0.06 to 0.26 and 0.30, respectively) more strongly than $^{147}Sm/^{144}Nd$ ratios (from 0.13 to 0.33 and 0.34, respectively), because the HREEs are compatible in garnet (e.g. van Westrenen et al., 1999). Consequently, the residue will evolve in time toward highly radiogenic Hf isotopes but more moderately radiogenic Nd isotopes. Eclogitic pyroxenite xenoliths in the Cretaceous Xuhuai plutons of the NCC do have such extreme Lu/Hf ratios and highly radiogenic Hf isotopes (Figure 9). Eventually, the residual eclogites with the decoupled Nd–Hf isotopic compositions remelted about 20 Ma (15% proportions of melts extracted), and mix with nearby peridotite-derived melts to produce the chain-related basalts in Shandong. The different arrays in the plot of ϵ_{Hf} vs. ϵ_{Nd} for the Shandong chain-related basalts and the Anfengshan basalts from the Sulu orogen can be accounted for if the recycled crust of their sources had undergone different-degree melting in the earlier stage (Figure 9).

As discussed above, the two-stage evolution model using recycled lower crustal material as the enriched end-member can well explain the mostly geochemical characteristics of these chain-related basalts. Here we found that such model is still successful to explain the lower Th/La ratios of these basalts (comparing with Dashan nephelinites and

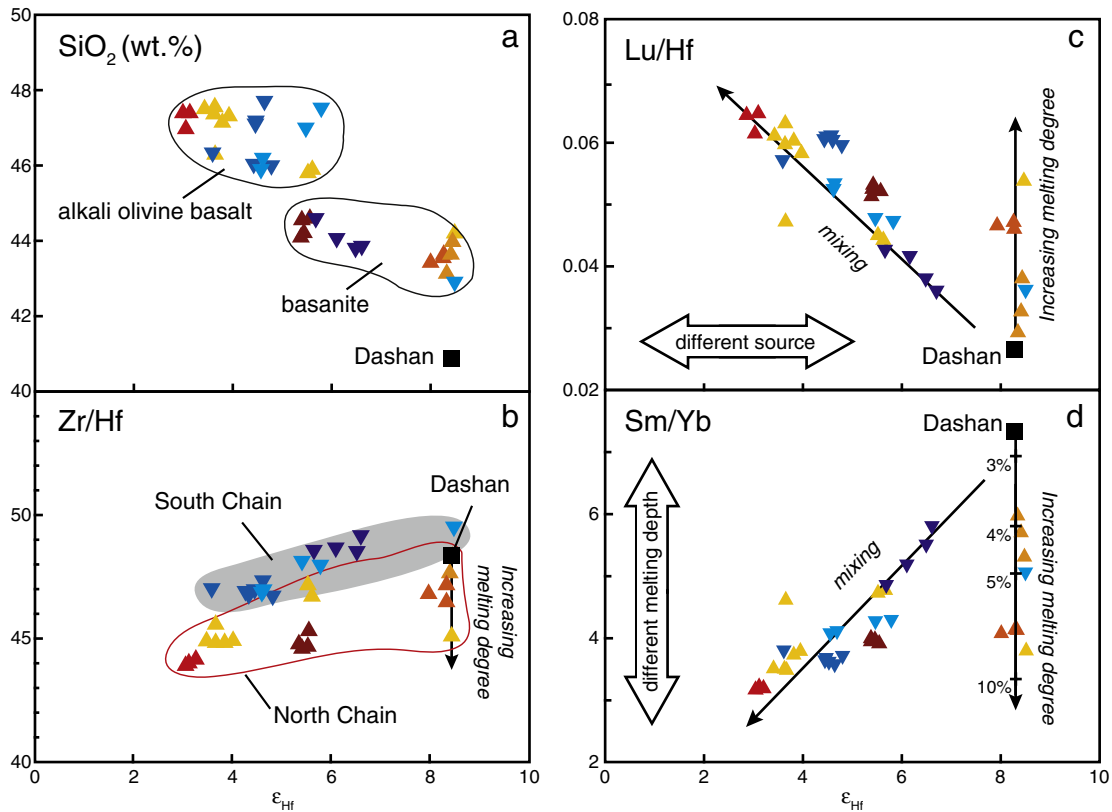


Fig. 7. Variations in SiO_2 , Zr/Hf, Lu/Hf and Sm/Yb vs. ϵ_{Hf} for chain-related basalts in Shandong. Dashan stands for the average values of Dashan nephelinites. Symbols are the same as in Figure 1b.

other alkaline rocks from isolated volcanoes in Shandong province), which have been used to rule out the potential influence of crustal contamination (Figure 5). Although the lower continental crust has higher Th/La ratio (0.15), the earlier melting (e.g. 60% proportions of melts extracted) of the recycled lower continental crust at 130 Ma can produce an eclogitic residue with low Th/La ratio (0.036). At 20 Ma, remelting of such residue can produce low-Th/La melts and lowered the Th/La ratios of these chain-related basalts in Shandong.

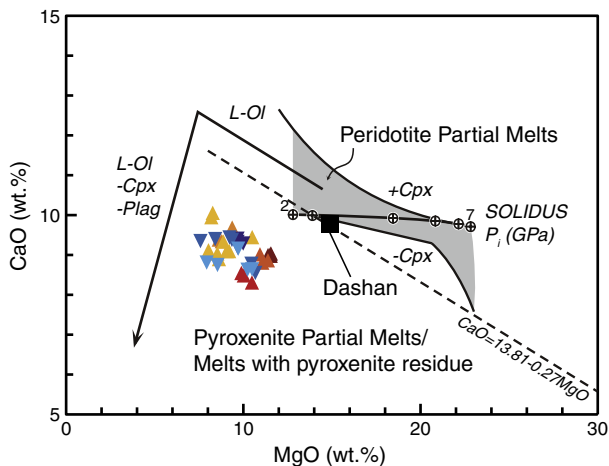


Fig. 8. Variations in CaO vs. MgO for chain-related basalts in Shandong. The broken line and the area for primary melts from peridotite are from Herzberg and Asimow (2008). Lavas with CaO contents lower than those defined by the broken line are potential pyroxenite partial melts. Dashan stands for the average values of Dashan nephelinites. Symbols for chain-related basalts in Shandong are the same as in Figure 1b.

4.3. Melting conditions for mantle sources

Basalts from the two volcanic chains show two arrays in the plots of Lu/Hf and Sm/Yb ratios vs. ϵ_{Hf} (Figure 6c, d). The first (correlated) array can be explained as mixing between residual eclogite-derived melts and carbonated peridotite-derived melts mentioned above, which are characterized by differences in both element and isotope ratios. Their enriched endmember(s) show higher Lu/Hf ratios and lower Sm/Yb ratios than their depleted endmember. On the contrary, the enriched endmember(s) of Anfengshan basalts from the Sulu orogenic belt nearby, which also have been proposed as melts derived from residual eclogite, have lower Lu/Hf ratios and higher Sm/Yb ratios than their depleted endmember (Chen et al., 2009a). The reversed correlations can be interpreted as different melting depth for eclogite. In the TLZ, the present thickness of the lithosphere is only ~60–70 km (Zheng et al., 2008), and new lithosphere has been accreted below the thinned lithosphere since Miocene (Xu, 2001), so the lithosphere thickness was <60 km at 20 Ma in this area. For the remelting of residual eclogite, garnet is unstable and is easier consumed than pyroxene in such a low-pressure condition (<60 km) (Prouteau et al., 2001; Rapp and Watson, 1995), and there is no garnet in the residue after the modest- to high-degree melting. Without the buffering of garnet, the enriched melts should be enriched in HREEs with high Lu/Hf ratios and low Sm/Yb ratios, and the recycled crust (eclogite) transformed into garnet-free pyroxenite. On the contrary, Anfengshan basalts are low-degree melts (Chen et al., 2009a) and should be derived from a deeper source. Remelting of such residual eclogite in different depth can be described as:

Residual eclogite → more depleted eclogite
 + high – Sm / Yb melts (garnet – stable depth)

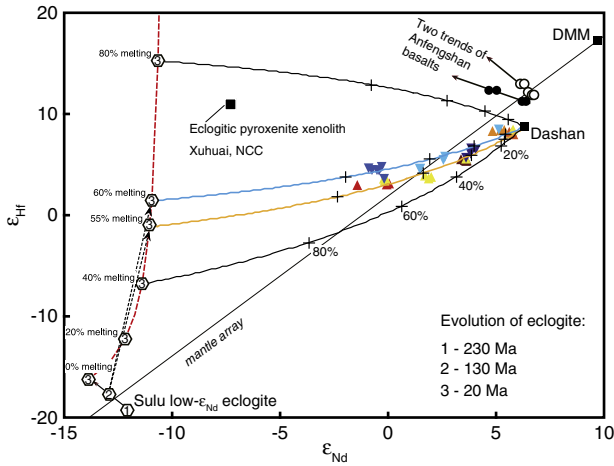


Fig. 9. Variations of ϵ_{Hf} vs. ϵ_{Nd} for chain-related basalts in Shandong and modeling for their genetic relationship. The average Nd–Hf isotopic values of Sulu low- ϵ_{Nd} eclogite are from Chen et al. (2009a). The average Nd–Hf isotopic values ($^{147}\text{Sm}/^{144}\text{Nd} = 0.16$, $^{143}\text{Nd}/^{144}\text{Nd} = 0.512258$; $^{176}\text{Lu}/^{177}\text{Hf} = 0.16$, $^{176}\text{Hf}/^{177}\text{Hf} = 0.283131$; average values of 11 samples) of eclogitic pyroxenite xenoliths in Xuhuai are from Xu et al. (2009) (Nd isotope) and unpublished data of S. Gao (Hf isotope), respectively. Dotted arrows represent the isotopic evolution of the eclogites after removal of partial melt 130 Ma ago. Red broken line stands for the trend of changed isotopic compositions for the eclogite (20 Ma) associated with different degree of partial melting 130 Ma ago. Different partial melting (55% and 60%) 130 Ma ago increased its $^{147}\text{Sm}/^{144}\text{Nd}$ (from 0.13 to 0.33 and 0.34, respectively) and $^{176}\text{Lu}/^{177}\text{Hf}$ ratios (from 0.06 to 0.26 and 0.30, respectively). At the time 20 Ma ago, such residues have decoupled Nd–Hf isotope values ($\epsilon_{\text{Nd}} = -11.1$, $\epsilon_{\text{Hf}} = -1.0$ for 55% early melting, and $\epsilon_{\text{Nd}} = -11.0$, $\epsilon_{\text{Hf}} = 1.4$ for 60% early melting, respectively). The two arrays of chain-related basalts from Shandong can be produced by mixing between peridotite-derived melts (represented by the average isotopic values of Dashan nephelinites) and the residual eclogite-derived melts (15% partial melting). Data for DMM is from Workman and Hart (2005). The partition coefficients for Lu, Hf, Sm are given by Klemme et al. (2002), the partition coefficients of clinopyroxene and garnet for Nd are from Pertermann and Hirschmann (2002) and Zack et al. (1997), respectively. The coefficients used are for garnet: Lu = 7.9, Hf = 0.31, Sm = 0.17, Nd = 0.02; for clinopyroxene: Lu = 0.63, Hf = 0.17, Sm = 0.30, Nd = 0.13. The proportions of residual phase during melting is assumed to be modal (with 40% garnet and 60% clinopyroxene in the first melting; 0% garnet and 100% clinopyroxene in the second melting). The mantle reference line is from Chauvel et al. (2008). The cycles stand for Anfengshan basalts from the Sulu orogen (Chen et al., 2009a). Dashan stands for the average values of Dashan nephelinites. Symbols for chain-related basalts in Shandong are the same as in Figure 1b.

Residual eclogite → garnet – free pyroxenite
+ low – Sm / Yb melts (garnet – unstable depth)

The other array shows variable element ratios but nearly constant isotopic composition, which is similar to that of Dashan nephelinites (Figure 6c, d). As shown by Zeng et al. (2010), La/Yb–Sm/Yb compositions of basalts can be used to estimate the melting degree, and the chain-related basalts from Shandong show variable degrees of melting from 3% to 10% (Figure 7d). Thus, the array with constant isotopic composition is likely to result from melting of carbonated peridotite in different degrees. In addition, the more silica-rich alkali olivine basalts show more enriched isotopic compositions than do basanites (Figure 7a), indicating greater contributions of eclogite-derived melts in the alkali olivine basalts.

4.4. Small-scale diversity between two volcanic chains

The isotopic compositions of basalts from the two volcanic chains show two slightly different mixing trends (Figure 6c, d). Such local differences are also seen in their Zr/Hf ratios (Figure 7b). Because the geochemical and isotopic signatures of each chain show rough correlations, each chain can be envisioned as consisting of two isotopically distinct endmember components, mixing in variable

proportions during melting. One of these endmembers is common to both mixing arrays. The differences between the enriched endmembers of the two chains reflect an additional, small-scale chemical and isotopic difference between the recycled crustal components in the respective mantle sources. These are explained by different proportions of melts extracted from eclogite during the first (Mesozoic) stage of evolution, and may indicate that the residual eclogite in the source of the south chain underwent the earlier melting in higher degree than that of the north chain. During the Cenozoic stage, the residual eclogite with different isotopic compositions melt and mix with nearby peridotite-derived melts to produce the trend of the chain-related basalts (Figure 9). The model outlined above is necessarily somewhat complex and cannot claim to be the unique, but it appears to be the simplest scenario that is consistent with all the geochemical observations.

4.5. Geodynamics: a lateral flow model

Several geodynamic mechanisms have been proposed to explain the wide-spread Cenozoic continental volcanism in NCC, including mantle upwelling in extensional setting with or without the subduction of Pacific plate (Huang and Zhao, 2006; Liu et al., 1992; Ren et al., 2002) and enhanced mantle temperature associated with plumes (Deng et al., 2004). The lack of any evidence for a subduction influence in the geochemical characteristics of early Tertiary to recent volcanic rocks rules out a dominant role of Pacific margin subduction (Menzies et al., 1993). In particular, the chain-related volcanoes in Shandong erupted in a narrow region near the TLFZ. These spatial relationships might indicate a genetic relationship between these basalts and the TLFZ, and are close to the extensional tectonics model proposed above. However, if these volcanic chains were controlled by the TLFZ, the direction of volcanic chains should be parallel to the TLFZ, which differs to the actual angle (40°) between the strike of the volcanic chains and the TLFZ. An alternative geodynamic model is still worthwhile to explore.

As discussed above, the geochemical data for alkaline basalts from the two volcanic chains have a bearing on the origin of mantle heterogeneities, and they specifically point to the involvement of recycled lower continental crust and a chemical fractionation event (loss of partial melt) in Mesozoic time, providing a sufficient time interval to develop the observed deviations from the normal terrestrial Nd–Hf isotope array. This type of residual crust (eclogite) has a higher density than peridotite (Jull and Kelemen, 2001; Rudnick and Fountain, 1995), and it seems unlikely to remain at a depth of shallow mantle from Mesozoic to Cenozoic. Therefore, we suggest that these crustal rocks were delaminated and transferred to greater depths in Mesozoic time, before being returned to the shallow mantle in Cenozoic time, when they remelted and mixed with asthenospheric (carbonated) peridotite-derived melts.

In addition, the differences between the two mixing trends resemble at least superficially the consistent isotopic differences between the so-called Loa- and Kea-trends observed in recent Hawaiian volcanism (Abouchami et al., 2000, 2005). Thus, if the Cenozoic upwelling resembled a deep-mantle plume, this plume might be expected to preserve local source differences, in a manner similar to those observed by Abouchami et al. (2005) and modeled by Farnetani and Hofmann (2010). These authors showed that locally persistent geochemical characteristics are best explained by stretching of heterogeneities into “filaments” in the plume conduit. These filaments may be further deformed and somewhat shortened when plume flow becomes subhorizontal beneath the lithosphere, but they should nevertheless retain their basic characteristics. Of course, this raises the question whether there is evidence for such a plume.

Recent high-resolution P wave tomography reveals that the subducted Pacific slab became stagnant in the mantle transition zone under eastern China, and the western end of the stagnant slab beneath the NCC reaches to approximately 119°E longitude (Huang

and Zhao, 2006). This observation means that the two volcanic chains in Shandong are located above the western edge of this stagnant slab. Beyond the barrier of the stagnant slab, warm material from the deep mantle might therefore move upward into the shallow mantle. However, the Shandong province is not the center of Cenozoic magmatism in the NCC, and Cenozoic magmatism in the Shandong Province is weaker than further to the west in Hannuoba and Datong. Therefore, if Cenozoic magmatism in the NCC is caused by a mantle plume, the plume is likely to be located under the central NCC rather than under the TLFZ. A recently observed low-velocity anomaly under the central NCC, which extends into the transition zone, supports such speculation (Zhao et al., 2009). Remarkably, Cenozoic basalts in the Taihang Mountain area, central NCC show a time-progressive trend from south to north, including Hebi (4.3–4.0 Ma), Zuoquan (5.6 Ma), Xiyang–Pingding (7.9–7.3 Ma) and Fansi (26–24 Ma) (Figure 1) (Liu et al., 1992; Tang et al., 2006). The hotspot-like distribution of these Cenozoic basalts in the Taihang Mountain area also supports the presence of a potential plume underneath the central NCC.

How can an underlying plume under the central NCC induce magmatism in the east NCC? The lateral flow model of plume material along the base of the lithosphere (e.g. Ebinger and Sleep, 1998; Sleep, 2002, 2006) can answer this question. Because the lithosphere of the eastern NCC (60–100 km) is much thinner than that of the central NCC (>120 km) (Chen et al., 2009b), the deep mantle material should flow from the central NCC toward the eastern NCC (Figure 10). Cenozoic basalts in the Taihang Mountain area show similar Sr–Nd isotopic compositions (Tang et al., 2006) to those of chain-related basalts in Shandong (Figure 6a, c), indicating a genetic relationship

between them, consistent with the above lateral flow model. When the plume-derived mantle material flows across the TLFZ, the thin lithosphere in this region (<60 km) would channel the ascending asthenospheric material (Figure 10) (Zheng et al., 2008). Consequently, the residual eclogite and nearby peridotite would melt simultaneously in the region of reduced pressure (induced by decreased lithospheric thickness), and thus produce the basalts from two parallel volcanic chains in Shandong.

5. Conclusion

The Cenozoic alkaline magmatism in Shandong consists of two parallel volcanic chains (24.0–10.3 Ma) and several isolated volcanoes (<10 Ma). For these chain-related basalts, correlations observed in the plots of $^{87}\text{Sr}/^{86}\text{Sr}$ vs. ϵ_{Nd} , and ϵ_{Nd} vs. ϵ_{Hf} suggest they represent mixtures of melts from three endmember mantle sources. The depleted component shows similar geochemical characteristics to Dashan nephelinites, suggesting an asthenospheric mantle source. The two enriched components have higher SiO_2 and lower Zr/Hf ratios, as well as decoupled Nd–Hf isotopic compositions, indicating the presence of ancient recycled lower continental crust in the source. In addition, systematic geochemical and isotopic differences between the two volcanic chains reflect an additional, small-scale diversity of the enriched component. To explain the involvement of old recycled crust and the small-scale diversity between two volcanic chains, we suggest a lateral flow model of deep mantle material (e.g. plume) along the base of the lithosphere as a geodynamic mechanism for the volcanic chains from Shandong. This mantle flow preserves local

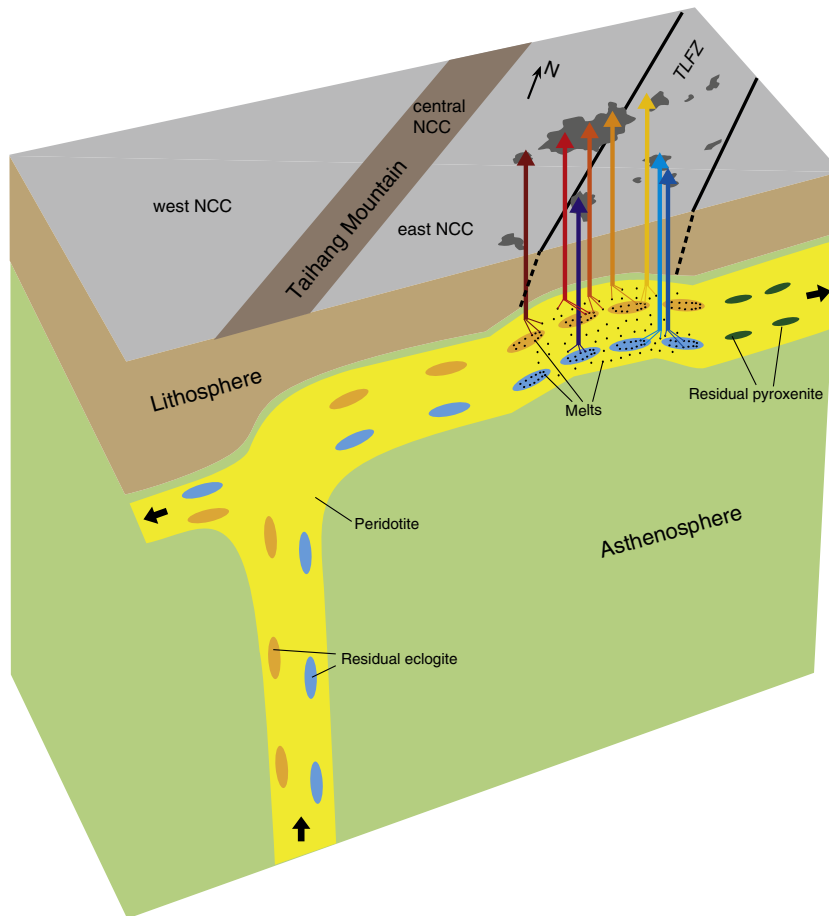


Fig. 10. Cartoon illustrating the genesis of basaltic volcanic chains in Shandong. Lenses of residual recycled crust (eclogites) are brought back to the upper mantle by a plume or an asthenospheric upwelling beneath central NCC. These deep mantle materials are then conveyed to the TLFZ by lateral asthenospheric flow along the base of lithosphere in the direction of lithospheric thinning. Consequently, the residual eclogites and nearby peridotite would melt simultaneously in such region of reduced pressure (induced by decreased lithospheric thickness), and thus produce the chain-related basalts in Shandong.

compositional differences, seen in these two volcanic chains, in a manner similar to the flow of the Hawaiian plume beneath the Pacific lithosphere, where it gives rise to consistent isotopic differences between the two parallel chains of volcanoes forming the Hawaiian islands.

Supplementary materials related to this article can be found online at doi:10.1016/j.epsl.2010.12.026.

Acknowledgements

We are grateful to Ye Liu, Yue-Heng Yang and Wei Pu for their technical support. Ji-Qiang Liu and Dan Luo attended the field investigations of this study. Shan Gao kindly provided the unpublished data. We are grateful to Liang Zhao and Ling Chen for discussions in geodynamics. We appreciate the thoughtful and constructive reviews provided by Editor Rick Carlson and the two anonymous reviewers. This study was supported by the National Natural Science Foundation of China (grant 40772035), the Chinese Ministry of Science and Technology (grant 2006CB403508) and the State Key Laboratory for Mineral Deposits Research (Nanjing University) (grants 2008-II-02 and 2009-II-7).

Appendix A. Analytical methods

Measurements of whole-rock major elements and trace elements were made at the Department of Geology, Northwest University, China. We used a RIX-2100 X-ray fluorescence spectrometer (XRF) to measure major elements. According to the measured values of standards (GSR-1 and GSR-3), the uncertainties are about $\pm 1\%$ for elements with concentrations >1.0 wt.%, and about $\pm 10\%$ for elements with concentrations <1.0 wt.%. Trace elements, including rare earth elements (REEs), were determined using an ELAN 6100DRC inductively coupled plasma mass spectrometer (ICP-MS) after acid digestion ($\text{HF} + \text{HNO}_3$) of samples in Teflon bombs. Analyses of USGS rock standards (BHVO-2, AGV-1, BCR-2, and G-2) indicate precision and accuracy better than 5% for Sc, V, Cr, Co, Ni, Rb, Sr, Y, Zr, Nb, Cs, Ba, Pb, U, and REEs, and 10% for Hf, Ta, and Th. The results of the analyses of these standards can be seen in Table S2.

Sr–Nd isotopic analyses were performed using a Finnigan Triton TI thermal ionization mass spectrometer at Nanjing University. Detailed analytical procedures for the Sr and Nd isotopic measurements are given by Pu et al. (2005). Sr and Nd isotopic compositions were normalized to $^{86}\text{Sr}/^{88}\text{Sr} = 0.1194$ and $^{146}\text{Nd}/^{144}\text{Nd} = 0.7219$. Measured values for the NBS987 Sr standard and JNdi-1 Nd standard were 0.710235 ± 0.000004 for $^{87}\text{Sr}/^{86}\text{Sr}$ and 0.512120 ± 0.000003 for $^{143}\text{Nd}/^{144}\text{Nd}$, respectively.

Hf isotopic data were obtained using a Neptune multicollector mass spectrometer at the Institute of Geology and Geophysics, Chinese Academy of Sciences. A detailed analytical procedure for the Hf isotopic measurement is given by Yang et al. (2010). Hf isotopic compositions were normalized to $^{179}\text{Hf}/^{177}\text{Hf} = 0.7325$, and the measured value for the W-2 and BHVO-2 Hf standard was 0.282702 ± 0.000008 and 0.283075 ± 0.000005 for $^{176}\text{Hf}/^{177}\text{Hf}$, respectively.

References

Abouchami, W., Galer, S., Hofmann, A., 2000. High precision lead isotope systematics of lavas from the Hawaiian Scientific Drilling Project. *Chem. Geol.* 169, 187–209.

Abouchami, W., Hofmann, A.W., Galer, S.J.G., Frey, F.A., Eisele, J., Feigenson, M., 2005. Lead isotopes reveal bilateral asymmetry and vertical continuity in the Hawaiian mantle plume. *Nature* 434, 851–856.

Chauvel, C., Lewin, E., Carpentier, M., Arndt, N.T., Marini, J.C., 2008. Role of recycled oceanic basalt and sediment in generating the Hf–Nd mantle array. *Nat. Geosci.* 1, 64–67.

Chen, L.H., Zeng, G., Jiang, S.Y., Hofmann, A.W., Xu, X.S., 2009a. Sources of Anfengshan basalts: subducted lower crust in the Sulu UHP belt, China. *Earth Planet. Sci. Lett.* 286, 426–435.

Chen, L., Cheng, C., Wei, Z., 2009b. Seismic evidence for significant lateral variations in lithospheric thickness beneath the central and western North China Craton. *Earth Planet. Sci. Lett.* 286, 171–183.

Chu, Z.Y., Wu, F.Y., Walker, R.J., Rudnick, R.L., Pitcher, L., Puchtel, I.S., Yang, Y.H., Wilde, S.A., 2009. Temporal evolution of the lithospheric mantle beneath the eastern North China Craton. *J. Petrol.* 50, 507–529.

Deng, J., Mo, X., Zhao, H., Wu, Z., Luo, Z., Su, S., 2004. A new model for the dynamic evolution of Chinese lithosphere: ‘continental roots-plume tectonics’. *Earth Sci. Rev.* 65, 223–275.

Ebinger, C.J., Sleep, N.H., 1998. Cenozoic magmatism throughout east Africa resulting from impact of a single plume. *Nature* 395, 788–791.

Farnetani, C.G., Hofmann, A.W., 2010. Dynamics and internal structure of the Hawaiian plume. *Earth Planet. Sci. Lett.* 295, 231–240.

Gao, S., Rudnick, R.L., Xu, W.-L., Yuan, H.L., Liu, Y.S., Walker, R.J., Puchtel, I.S., Liu, X., Huang, H., Wang, X.-R., Yang, J., 2008. Recycling deep cratonic lithosphere and generation of intraplate magmatism in the North China Craton. *Earth Planet. Sci. Lett.* 270, 41–53.

Gao, S., Rudnick, R.L., Yuan, H.L., Liu, X.M., Liu, Y.S., Xu, W.L., Ling, W.L., Ayers, J., Wang, X.C., Wang, Q.H., 2004. Recycling lower continental crust in the North China craton. *Nature* 432, 892–897.

Herzberg, C., 2006. Petrology and thermal structure of the Hawaiian plume from Mauna Kea volcano. *Nature* 444, 605–609.

Herzberg, C., Asimow, P.D., 2008. Petrology of some oceanic island basalts: PRIMELT2. XLS software for primary magma calculation. *Geochem. Geophys. Geosyst.* 9. doi:10.1029/2008gc002057.

Hirschmann, M.M., Kogiso, T., Baker, M.B., Stolper, E.M., 2003. Alkalic magmas generated by partial melting of garnet pyroxenite. *Geology* 31, 481–484.

Hofmann, A.W., Jochum, K.P., Seufert, M., White, W.M., 1986. Nb and Pb in oceanic basalts: new constraints on mantle evolution. *Earth Planet. Sci. Lett.* 79, 33–45.

Huang, J.L., Zhao, D.P., 2006. High-resolution mantle tomography of China and surrounding regions. *J. Geophys. Res.* 111. doi:10.1029/2005JB004066.

Jahn, B., Wu, F., Lo, C.H., Tsai, C.H., 1999. Crust–mantle interaction induced by deep subduction of the continental crust: geochemical and Sr–Nd isotopic evidence from post-collisional mafic–ultramafic intrusions of the northern Dabie complex, central China. *Chem. Geol.* 157, 119–146.

Jull, M., Kelemen, P., 2001. On the conditions for lower crustal convective instability. *J. Geophys. Res.* 106, 6423–6446.

Klemme, S., Blundy, J.D., Wood, B.J., 2002. Experimental constraints on major and trace element partitioning during partial melting of eclogite. *Geochim. Cosmochim. Acta* 66, 3109–3123.

Kogiso, T., Hirschmann, M.M., Frost, D.J., 2003. High-pressure partial melting of garnet pyroxenite: possible mafic lithologies in the source of ocean island basalts. *Earth Planet. Sci. Lett.* 216, 603–617.

Kogiso, T., Hirschmann, M.M., 2006. Partial melting experiments of bimineralic eclogite and the role of recycled mafic oceanic crust in the genesis of ocean island basalts. *Earth Planet. Sci. Lett.* 249, 188–199.

Le Bas, M., Le Maitre, R., Streckeisen, A., Zanettin, B., 1986. A chemical classification of volcanic rocks based on the total alkali–silica diagram. *J. Petrol.* 27, 745–750.

Liu, R.X., Chen, W.J., Sun, J.Z., Li, D.M., 1992. The K–Ar age and tectonic environment of Cenozoic volcanic rocks in China. In: Liu, R.X. (Ed.), *The Age and Geochemistry of Cenozoic Volcanic Rock in China*. Seismology Publ., Beijing, pp. 1–43 (in Chinese).

Liu, Y.S., Gao, S., Kelemen, P.B., Xu, W.L., 2008. Recycled crust controls contrasting source compositions of Mesozoic and Cenozoic basalts in the North China Craton. *Geochim. Cosmochim. Acta* 72, 2349–2376.

Luo, D., Chen, L.H., Zeng, G., 2009. Genesis of intra-continental strongly alkaline volcanic rocks: a case study of Dashan nephelinites in Wudi, Shandong Province. *N. China. Acta Petrol. Sin.* 25, 311–319 (in Chinese).

McDonough, W.F., Sun, S.S., 1995. The composition of the Earth. *Chem. Geol.* 120, 223–253.

Menzies, M.A., Fan, W.M., Zhang, M., 1993. Palaeozoic and Cenozoic lithoprobes and the loss of >120 km of Archaean lithosphere, Sino-Korean craton, China. In: Prichard, H.M., Alabaster, T., Harris, N.B.W., Neary, C.R. (Eds.), *Magmatic Processes and Plate Tectonics*: Geo. Soc. London Sp. Pub., pp. 71–78.

Peng, Z.C., Zartman, R.E., Futa, K., Chen, D.G., 1986. Pb-, Sr- and Nd-isotopic systematics and chemical characteristics of Cenozoic basalts, eastern China. *Chem. Geol.* 59, 3–33.

Pertermann, M., Hirschmann, M.M., 2002. Trace-element partitioning between vacancy-rich eclogitic clinopyroxene and silicate melt. *Am. Mineral.* 87, 1365–1376.

Pertermann, M., Hirschmann, M.M., 2003a. Anhydrous partial melting experiment on MORB-like eclogites phase relations, phase composition and mineral-melt partitioning of major elements at 2–3 GPa. *J. Petrol.* 44, 2173–2202.

Pertermann, M., Hirschmann, M.M., 2003b. Partial melting experiments on a MORB-like pyroxenite between 2 and 3 GPa: constraints on the presence of pyroxenite in basalt source regions from solidus location and melting rate. *J. Geophys. Res.* 108, 2125–2142.

Plank, T., Langmuir, C.H., 1998. The chemical composition of subducting sediment and its consequences for the crust and mantle. *Chem. Geol.* 145, 325–394.

Prouteau, G., Scaillet, B., Pichavant, M., Maury, R., 2001. Evidence for mantle metasomatism by hydrous silicic melts derived from subducted oceanic crust. *Nature* 410, 197–200.

Pu, W., Gao, J.F., Zhao, K.D., Lin, H.F., Jiang, S.Y., 2005. Separation method of Rb–Sr, Sm–Nd using DCTA and HIBA. *J. Nanjing Univ. (Nat. Sci.)* 41, 445–450 (in Chinese).

Rapp, R.P., Watson, E.B., 1995. Dehydration melting of metabasalt at 8–32 kbar: implications for continental growth and crust–mantle recycling. *J. Petrol.* 36, 891–931.

- Ren, J., Tamaki, K., Li, S., Junxia, Z., 2002. Late Mesozoic and Cenozoic rifting and its dynamic setting in Eastern China and adjacent areas. *Tectonophysics* 344, 175–205.
- Rudnick, R., Fountain, D., 1995. Nature and composition of the continental crust: a lower crustal perspective. *Rev. Geophys.* 33, 267–309.
- Rudnick, R.L., Gao, S., 2003. Composition of the continental crust. In: Rudnick, R.L. (Ed.), *Treatise on Geochemistry*. Elsevier, pp. 1–64.
- Shandong Institute of Geological Survey, 2005. 1:250000 Geological Map (Weifang Scope). (in Chinese).
- Sleep, N.H., 2002. Local lithospheric relief associated with fracture zones and ponded plume material. *Geochem. Geophys. Geosyst.* 3. doi:10.1029/2001GC000290.
- Sleep, N.H., 2006. Mantle plumes from top to bottom. *Earth Sci. Rev.* 77, 231–271.
- Song, Y., Frey, F.A., Zhi, X., 1990. Isotopic characteristics of Hannuoba basalts, eastern China: implications for their petrogenesis and the composition of subcontinental mantle. *Chem. Geol.* 88, 35–52.
- Tang, Y.J., Zhang, H.F., Ying, J.F., 2006. Asthenosphere–lithospheric mantle interaction in an extensional regime: implication from the geochemistry of Cenozoic basalts from Taihang Mountains, North China Craton. *Chem. Geol.* 233, 309–327.
- van Westrenen, W., Blundy, J., Wood, B., 1999. Crystal–chemical controls on trace element partitioning between garnet and anhydrous silicate melt. *Am. Mineral.* 84, 838–847.
- Workman, R.K., Hart, S.R., 2005. Major and trace element composition of the depleted MORB mantle (DMM). *Earth Planet. Sci. Lett.* 231, 53–72.
- Xiao, Y., Zhang, H.F., Fan, W.M., Ying, J.F., Zhang, J., Zhao, X.M., Su, B.X., 2010. Evolution of lithospheric mantle beneath the Tan-Lu fault zone, eastern North China Craton: evidence from petrology and geochemistry of peridotite xenoliths. *Lithos* 117, 229–246.
- Xu, W.L., Gao, S., Yang, D.B., Pei, F.P., Wang, Q.H., 2009. Geochemistry of eclogite xenoliths in Mesozoic adakitic rocks from Xuzhou–Suzhou area in central China and their tectonic implications. *Lithos* 107, 269–280.
- Xu, Y.-G., 2001. Thermo-tectonic destruction of the Archean lithospheric keel beneath the Sino-Korean craton in China: evidence, timing and mechanism. *Phys. Chem. Earth A* 26, 747–757.
- Xu, Y.G., Ma, J.L., Frey, F.A., Feigenson, M.D., Liu, J.F., 2005. Role of lithosphere–asthenosphere interaction in the genesis of Quaternary alkali and tholeiitic basalts from Datong, western North China Craton. *Chem. Geol.* 224, 247–271.
- Yang, Y.H., Zhang, H.F., Chu, Z.Y., Xie, L.W., Wu, F.Y., 2010. Combined chemical separation of Lu, Hf, Rb, Sr, Sm and Nd from a single rock digest and precise and accurate isotope determinations of Lu–Hf, Rb–Sr and Sm–Nd isotope systems using Multi-Collector ICP-MS and TIMS. *Int. J. Mass Spectrom.* 290, 120–126.
- Yaxley, G.M., Green, D.H., 1998. Reactions between eclogite and peridotite: mantle refertilisation by subduction of oceanic crust. *Schweiz. Mineral. Petrogr. Mitt.* 78, 243–255.
- Zack, T., Foley, S.F., Jenner, G.A., 1997. A consistent partition coefficient set for clinopyroxene, amphibole and garnet from laser ablation microprobe analysis of garnet pyroxenites from Kakanui, New Zealand. *Neues Jahrb. Mineral. Abh.* 172, 23–41.
- Zeng, G., Chen, L.H., Xu, X.S., Jiang, S.Y., Hofmann, A.W., 2010. Carbonated mantle sources for Cenozoic intra-plate alkaline basalts in Shandong, North China. *Chem. Geol.* 273, 35–45.
- Zhang, H.F., Sun, M., Zhou, X.H., Fan, W.M., Zhai, M.G., Yin, J.F., 2002. Mesozoic lithosphere destruction beneath the North China Craton: evidence from major-, trace-element and Sr–Nd–Pb isotope studies of Fangcheng basalts. *Contrib. Mineral. Petrol.* 144, 241–254.
- Zhang, J.J., Zheng, Y.F., Zhao, Z.F., 2009. Geochemical evidence for interaction between oceanic crust and lithospheric mantle in the origin of Cenozoic continental basalts in east-central China. *Lithos* 110, 305–326.
- Zhao, G.C., Sun, M., Wilde, S.A., Li, S.Z., 2005. Late Archean to Paleoproterozoic evolution of the North China Craton: key issues revisited. *Precambrian Res.* 136, 177–202.
- Zhao, L., Allen, R.M., Zheng, T.Y., Hung, S.H., 2009. Reactivation of an Archean craton: constraints from P- and S-wave tomography in North China. *Geophys. Res. Lett.* 36. doi:10.1029/2009GL039781.
- Zheng, T.Y., Zhao, L., Xu, W.W., Zhu, R.X., 2008. Insight into modification of North China Craton from seismological study in the Shandong Province. *Geophys. Res. Lett.* 35. doi:10.1029/2008GL035661.
- Zindler, A., Hart, S., 1986. Chemical geodynamics. *Annu. Rev. Earth Planet. Sci.* 14, 493–571.
- Zou, H.B., Zindler, A., Xu, X.S., Qi, Q., 2000. Major, trace element, and Nd, Sr and Pb isotope studies of Cenozoic basalts in SE China: mantle sources, regional variations, and tectonic significance. *Chem. Geol.* 171, 33–47.